

Evolution of Polyoxoniobate Cluster Anions**

Ranko P. Bontchev and May Nyman*

Early transition metals such as V, Mo, and W are well known to form complex polyoxoanions over a wide pH range,^[1] for example, some exceptionally large ring-shaped oxo-molybdenum clusters that contain up to several hundred metal centers.^[2] In contrast, polyoxoniobates can be stabilized only under basic conditions, and their chemistry was initially dominated by the hexaniobate Lindqvist anion $[\text{Nb}_6\text{O}_{19}]^{8-}$ in solution and by its alkali salts in the solid state.^[3] More recently, the dodecaniobate Keggin ion $[\text{TNb}_{12}\text{O}_{40}]^{16-}$ (T = Si, Ge, P) and its lacunary derivatives were also synthesized by using hydrothermal processing and slightly lower alkalinity.^[4] The isolation of alternative polyoxoniobate cluster types in the solid state, especially through nonhydrothermal synthetic routes, has been hindered by the narrow working pH range (10.5–12.5) and the pervasiveness of the oxido-niobium Lindqvist and Keggin ions. The only other polyoxoniobate clusters known to date are $[\text{Nb}_{10}\text{O}_{28}]^{6-}$,^[5a] its structural analogue $[\text{Ti}_2\text{Nb}_8\text{O}_{28}]^{8-}$,^[5b] and the dimeric derivative $[\text{Nb}_{20}\text{O}_{54}]^{8-}$.^[5c] The unique characteristics of the polyoxoniobate family (high charge/surface ratio and basicity) justify further exploration of potential practical applications in virology,^[6a] nuclear-waste treatment,^[4c,6b,c] and the base-catalyzed decomposition of biocontaminants.^[6d]

Herein we report the synthesis and crystal structure of a new polyoxoniobate cluster type $[\text{Nb}_{24}\text{O}_{72}\text{H}_9]^{15-}$ (**1**). To the best of our knowledge, **1** has no analogues among the known polyoxometalate cluster geometries and is the largest isopolyniobate cluster reported to date. We also show that its structure could be derived from two fundamental structural

types (Figure 1) and that **1** may serve as a building block for even larger clusters and extended structures.

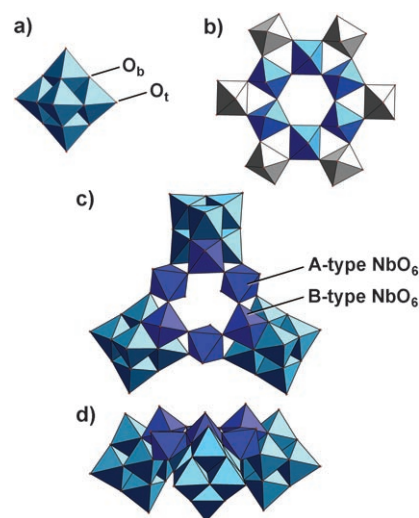


Figure 1. a) The Lindqvist anion $[\text{Nb}_6\text{O}_{19}]^{8-}$; O_b and O_t depict bridging (Nb– O_b –Nb) and terminal (Nb– O_t) oxygen atoms, respectively; b) the cyclic $\{\text{Nb}_6\text{O}_{30}\}$ unit (dark blue) in the pyrochlore frameworks $\text{HNbO}_3 \cdot 0.5\text{H}_2\text{O}$ and $\text{RbNb}_2\text{O}_5\text{F}$ (gray);^[8] c) top view of the cluster anion $[\text{Nb}_{24}\text{O}_{72}\text{H}_9]^{15-}$ (**1**) consisting of three Lindqvist $[\text{Nb}_6\text{O}_{19}\text{H}_x]$ clusters (light blue) linked by a cyclic $\{\text{Nb}_6\text{O}_{30}\text{H}_{9-x}\}$ cluster (dark blue); d) side view of **1**.

The reaction of rubidium hexaniobate, copper(II) nitrate, ethylenediamine (en), and water at near-ambient temperature yielded crystals of $(\text{H}_2\text{en})_6[\text{Cu}(\text{en})_2(\text{H}_2\text{O})_2]_3 \cdot [(\text{Nb}_{24}\text{O}_{72}\text{H}_9)\{\text{Cu}(\text{en})_2(\text{H}_2\text{O})\}_2\{\text{Cu}(\text{en})_2\}_2] \cdot 66\text{H}_2\text{O}$ (**2**).^[7] The new cluster anion **1** is shown in Figure 1 c. It can be described as three Lindqvist $\{\text{Nb}_6\text{O}_{19}\}$ clusters linked together by a cyclic $\{\text{Nb}_6\text{O}_{30}\}$ cluster. The same $\{\text{Nb}_6\text{O}_{30}\}$ structural motif is found in Nb-based solids of the pyrochlore type, such as $\text{HNbO}_3 \cdot 0.5\text{H}_2\text{O}$ and $\text{RbNb}_2\text{O}_5\text{F}$ (Figure 1 b).^[9] The $\{\text{Nb}_6\text{O}_{30}\}$ ring consists of six NbO_6 octahedra sharing common (μ_2 -O) corners. Three of these NbO_6 octahedra (A-type NbO_6) link two adjacent $[\text{Nb}_6\text{O}_{19}]$ clusters through corner atoms, and the remaining three (B-type) NbO_6 octahedra each share three edges with a Lindqvist cluster (Figure 1 c). The B-type NbO_6 octahedron is also bonded to the face of the Lindqvist superoctahedron and hence together may be alternatively described as a heptaniobate cluster.

A number of differentiating structural features of the $\{\text{Nb}_6\text{O}_{30}\}$ ring in **1** emerge in comparison with the pyrochlore motif ($\text{Nb}_6\text{O}_{24}\text{F}_6$) mentioned above.^[9] The NbO_6 octahedra in the pyrochlore motif are only slightly tilted with respect to each other (Figure 1 b). In comparison, the A-type NbO_6 octahedra in **1** are considerably more tilted and their O_t –Nb– O_t axes (Nb– $\text{O}_t \approx 1.75$ Å, *trans*-Nb– $\text{O}_t \approx 2.45$ Å) point almost parallel to the equatorial plane of the ring (Figure 1 c, d). Another significant difference is the presence of *trans* terminal (μ_1 - O_t) oxygen atoms in each A-type NbO_6 octahedron in **1** (Figure 1 c). In contrast, all O/F atoms in the pyrochlore motif are bridging (μ_2 -type), all occupy one crystallographically independent position, and the Nb–O(F)

[*] Dr. R. P. Bontchev, Dr. M. Nyman
Sandia National Laboratories
P.O. Box 5800, MS 0754, Albuquerque, NM 87185-0754 (USA)
Fax: (+1) 505-844-7354
E-mail: mdnyman@sandia.gov

[**] Sandia is a multiprogram laboratory operated by Sandia Corporation, a Lockheed Martin Company, for the United States Department of Energy's National Nuclear Security Administration under contract DE-AC04-94AL85000. This work was supported by Sandia National Laboratories' Laboratory Directed Research and Development (LDRD) program. We thank Dr. M. Iliev (Texas Center for Superconductivity and Advanced Materials, Houston, Texas) for the Raman analyses. We thank Reference Metals, Inc. (CBMM, Araxá, Brazil) for the generous gift of hydrous niobium. We cite to the definition of "evolution" from the Merriam-Webster dictionary as "a process of continuous change from a lower, simpler to a higher, more complex state" in reference to the assembly of more-complex structures from simpler building blocks.

Supporting information (table comparing Nb–O bond lengths for **1**, protonated and nonprotonated $\{\text{Nb}_6\text{O}_{19}\}$ Lindqvist ions, and pyrochlore) for this article is available on the WWW under <http://www.angewandte.org> or from the author.

bond lengths are equal and on the order of 2.0 Å (see the Supporting Information).^[9] All six short Nb=O bonds in the {Nb₆O₃₀} ring are located on the same side with respect to the equatorial plane of the Nb₆ ring (Figure 1 c), and the same is also true for their long *trans*-oriented Nb–O counterparts.

Charge-balance considerations of **2** dictate that there must be nine protons per {Nb₂₄O₇₂} unit (i.e., {Nb₂₄O₇₂H₉}^{15–}). The very high number of crystallographically independent atoms and variable parameters prevented direct location of the protons from the Fourier maps.^[7] Bond-valence calculations did not provide an obvious solution as a result of atypical distortions and the relatively wide variation of the Nb–O bond lengths.^[10] These bond lengths are summarized and compared with those of protonated Rb₈[Nb₆O₁₉H₂]·9H₂O and nonprotonated Rb₈[Nb₆O₁₉]·14H₂O Lindqvist clusters in the Supporting Information.^[3c] The typical lengthening of the Nb–μ₂-OH bonds in protonated {Nb₆O₁₉} clusters is further masked by additional distortions that result from the linking of the {Nb₆O₁₉} and {Nb₆O₃₀} units, which makes the unambiguous assignment of the protonated oxygen atoms in **1** challenging. Neutron-diffraction studies have shown that the protons in HNbO₃·0.5H₂O, HTaWO₆, and HTaWO₆·H₂O pyrochlores are present as framework hydroxy groups.^[9a] The three long Nb–O_i bonds (2.27–2.45 (1) Å) of the A-type NbO₆ octahedra in {Nb₆O₃₀} (Figure 1 b,c) indicate the most obvious sites for protonation. Bond valence sum (BVS) calculations gave values of 0.2–0.3 for each of these Nb–O_i terminal oxygen atoms.^[10] The expected oxygen BVS of 2 could be completed by assuming a hydrogen atom at bonding distance of 0.7–0.8 Å.

In several earlier infrared and Raman studies of {Nb₆O₁₉}, the bands corresponding to terminal Nb–O_i and bridging Nb–O_b–Nb vibrations were identified and assigned as Nb–O_i > 800 cm^{–1} and 400 < Nb–O_b–Nb < 750 cm^{–1}.^[11] In our FTIR and Raman studies on Rb₈[Nb₆O₁₉]·14H₂O, Rb₆[Nb₆O₁₉H₂]·9H₂O, and **2**, we observed systematic and measurable shifts towards higher energies of the same bands in the spectra of the protonated clusters relative to the nonprotonated clusters (see the Experimental Section). This observation indicates that the same types of oxygen atoms (bridging) of the Lindqvist ions in **1** are most probably protonated. This conclusion is also in accordance with recent structural studies on protonated Lindqvist salts such as Rb₆[Nb₆O₁₉H₂]·14H₂O which showed that the protons are associated with two adjacent bridging (μ₂-O) sites.^[3c] Even stronger evidence comes from the structural characterization of several related {Cu(en)₂}²⁺-linked {Nb₆O₁₉H₂} phases that feature the same doubly protonated cluster faces.^[3b] All of the above evidence strongly suggests that six of the nine protons in **1** are located as neighboring μ₂-O_bH pairs on the three Lindqvist units and the other three are on the oxygen atoms of the three long terminal Nb–O_i bonds of the A-type NbO₆ octahedra of the {Nb₆O₃₀} ring.

Each {Nb₂₄O₇₂H₉}^{15–} cluster is “decorated” by two terminal {Cu(en)₂(H₂O)} units with Cu–N bond lengths ranging between 1.90(1) and 2.17(1) Å (Figure 2). One is connected to the O_i oxygen atom of the A-type NbO₆ octahedron with Cu–O_i = 2.30 (1) Å and Cu–OH₂ = 2.71(1) Å. The second {Cu(en)₂(H₂O)} unit is connected to a bridging (μ₂-O_b)

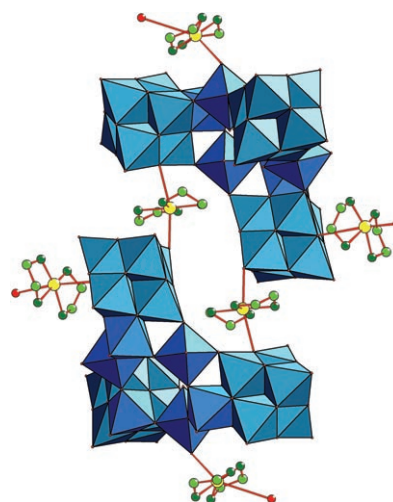


Figure 2. The dimer $[(\{Nb_{24}O_{72}H_9\}\{Cu(en)_2(H_2O)\}_2\{Cu(en)_2\})_2]^{18-}$. The clusters of **1** are shown in blue; copper, oxygen, carbon, and nitrogen atoms are shown as yellow, red, and light- and dark-green spheres, respectively.

oxygen atom from the diametrically opposite [Nb₆O₁₉] Lindqvist unit with bond lengths of Cu–O_b = 2.36(1) Å and Cu–OH₂ = 2.71(1) Å (Figure 2). A pair of {Nb₂₄O₇₂H₉}{Cu(en)₂(H₂O)}₂ clusters are linked together by two {Cu(en)₂} bridges through one terminal oxygen atom (Cu–O_i = 2.47(1) Å) and one bridging oxygen atom (Cu–O_b = 2.67(1) Å) from Lindqvist units on adjacent clusters of **1** to form dimers $[(\{Nb_{24}O_{72}H_9\}\{Cu(en)_2(H_2O)\}_2\{Cu(en)_2\})_2]^{18-}$ (Figure 2). The remaining overall charge balance is provided by isolated, disordered [Cu(en)₂(H₂O)₂]²⁺ complexes and (H₂en)²⁺ molecules, which, together with water molecules, fill the space between the clusters. An extended network of O–H···O hydrogen bonds between all of the lattice species provides the 3D connectivity in the overall structure.

Although not unique to polyoxometalates,^[12] the fact that the counteranions in **2** are charged copper complexes and protonated organic species is quite unusual for polyoxoniobates. All of the structurally characterized Lindqvist-based clusters to date are charge compensated only by alkali cations, which generally have higher charge density than organic cations.^[3] It is tempting to assume that in polyoxoniobate chemistry, large cations with relatively low charge density similar to [CuL_x]²⁺ favor the formation of larger clusters such as **1**. Supporting this idea is the fact that the only other structurally characterized polyoxoniobates different from the Lindqvist or Keggin anions, namely [Nb₁₀O₂₈]^{6–} and [Nb₂₀O₅₄]^{8–}, have been also isolated by using low-charge-density cations (tetramethyl- and tetrabutylammonium, respectively).^[5a,c] All these considerations suggest that the use of organic cations or metal–ligand cations could provide new avenues towards diversification of polyoxoniobate cluster geometries, as well as an insight in their non-aqueous chemistry.

In conclusion, we have followed the structural evolution of the simple NbO₆ octahedron to two basic structural units—the Lindqvist [Nb₆O₁₉] and the pyrochlore cyclic {Nb₆O₃₀} clusters. We have demonstrated that their combination results

in the unique polyoxoniobate cluster anion $\{\text{Nb}_{24}\text{O}_{72}\text{H}_9\}^{15-}$ (**1**), the $\{\text{Cu}(\text{en})_2(\text{H}_2\text{O})\}$ -coordinated species, the dimer $[(\{\text{Nb}_{24}\text{O}_{72}\text{H}_9\}\{\text{Cu}(\text{en})_2(\text{H}_2\text{O})\})_2\{\text{Cu}(\text{en})_2\}]^{18-}$, and finally the complex overall 3D structure of **2**. Synthetic studies towards related polyoxoniobate-counterion systems are currently under way.

Experimental Section

Synthesis of **2**: Rubidium hexaniobate was synthesized as previously reported.^[3c] $\text{Rb}_8\text{Nb}_6\text{O}_{19}\cdot 14\text{H}_2\text{O}$ (0.95 g, 0.5 mmol), $\text{Cu}(\text{NO}_3)_2\cdot 2.5\text{H}_2\text{O}$ (0.48 g, 2.0 mmol), ethylenediamine (10 g, 167 mmol), and water (10 g, 550 mmol) were mixed in a 50-mL beaker by stirring at 60 °C for 30 min. The beaker was covered with parafilm and left at room temperature. Prismatic deep-purple crystals up to 0.5 mm in size began forming at the bottom of the beaker after 3 days. After 5 days, the sample was filtered, and a few crystals were selected for single-crystal X-ray diffraction analysis. Elemental analysis (Galbraith Laboratories, Inc.): expected formula (XRD) $(\text{Cu}_{4.5}\text{Nb}_{24}\text{C}_{24}\text{N}_{24}\text{O}_{77}\text{H}_{151})\cdot 33\text{H}_2\text{O}$; found $(\text{Cu}_{4.34}\text{Nb}_{24.29}\text{C}_{23.73}\text{N}_{23.39}\text{H}_{150.91})\cdot 18\text{H}_2\text{O}$; the difference in the number of water molecules of crystallization is due to prolonged storage. Infrared spectra were recorded on a Perkin Elmer Spectrum One spectrometer within the range 400–4000 cm^{-1} as KBr pellets. Raman spectra were measured by using the Ar^+ laser line (488.0 nm) and a CCD single spectrometer (spot diameter 5–7 μm , 0.6 mW, average laser power density of 1000–2000 W cm^{-2}). IR: **2**: $\tilde{\nu} = 530\text{s}, 704\text{s}, 751\text{s}, 848\text{s cm}^{-1}$; $\text{Rb}_8[\text{Nb}_6\text{O}_{19}]\cdot 14\text{H}_2\text{O}$: $\tilde{\nu} = 523\text{s}, 691\text{s}, 736\text{s}, 825\text{s cm}^{-1}$; $\text{Rb}_6[\text{Nb}_6\text{O}_{19}\text{H}_2]\cdot 9\text{H}_2\text{O}$: $\tilde{\nu} = 531\text{s}, 969\text{s}, 749\text{s}, 867\text{s cm}^{-1}$. Raman: **2**: $\tilde{\nu} = 480\text{s}, 533\text{s}, 561\text{s}, 816\text{m}, 856\text{m}, 897\text{vs cm}^{-1}$; $\text{Rb}_8[\text{Nb}_6\text{O}_{19}]\cdot 14\text{H}_2\text{O}$: $\tilde{\nu} = 463, 536, 828\text{m}, 876\text{vs cm}^{-1}$; $\text{Rb}_6[\text{Nb}_6\text{O}_{19}\text{H}_2]\cdot 9\text{H}_2\text{O}$: $\tilde{\nu} = 474\text{s}, 536\text{s}, 556\text{s}, 820\text{m}, 848\text{m}, 892\text{vs cm}^{-1}$.

Received: June 2, 2006

Revised: August 8, 2006

Published online: September 20, 2006

Keywords: cluster compounds · niobium · polyoxometalates · solid-state structures

- [1] a) M. T. Pope, *Heteropoly and Isopoly Oxometalates*, Springer, New York, **1983**; b) M. T. Pope, A. Müller, *Angew. Chem.* **1991**, *103*, 56; *Angew. Chem. Int. Ed. Engl.* **1991**, *30*, 34; c) W. G. Klemperer, T. A. Marquart, O. M. Yaghi, *Angew. Chem.* **1992**, *104*, 51; *Angew. Chem. Int. Ed. Engl.* **1992**, *31*, 49.
- [2] a) A. Müller, E. Krickemeyer, H. Bögge, M. Schmidtman, C. Beugholt, P. Kögerler, C. Lu, *Angew. Chem.* **1998**, *110*, 1278; *Angew. Chem. Int. Ed.* **1998**, *37*, 1220; b) A. Müller, M. Koop, H. Bögge, M. Schmidtman, C. Beugholt, *Chem. Commun.* **1998**, 1501; c) C.-C. Jiang, Y.-G. Wei, Q. Liu, S.-W. Zhang, M.-C. Shao, Y.-Q. Tang, *Chem. Commun.* **1998**, 1937; d) A. Müller, S. Q. N. Shah, H. Bögge, M. Schmidtman, *Nature* **1999**, *397*, 48; e) A. Müller, P. Kögerler, A. W. M. Dress, *Coord. Chem. Rev.* **2001**, *222*, 193; f) B. Botar, P. Kögerler, C. L. Hill, *J. Am. Chem. Soc.* **2006**, *128*, 5336.
- [3] a) I. Lindqvist, *Ark. Kemi* **1953**, *5*, 247; b) A. Goiffon, E. Philippot, M. Maurin, *Rev. Chim. Miner.* **1980**, *17*, 466; c) M. Nyman, T. M. Alam, F. Bonhomme, M. A. Rodriguez, C. S. Frazer, M. E. Welk, *J. Cluster Sci.* **2006**, *17*, 197; d) M. Müller, *Rev. Chim. Miner.* **1970**, *7*, 359; e) G. M. Rozantsev, O. I. Dotsenko, G. V. Taradina, *Russ. J. Coord. Chem.* **2000**, *26*, 247; f) T. M. Alam, M. Nyman, B. R. Cherry, J. M. Segall, L. E. Lybarger, *J. Am. Chem. Soc.* **2004**, *126*, 5610; g) T. Ozeki, T. Yamase, H. Naruke, Y. Sasaki, *Bull. Chem. Soc. Jpn.* **1994**, *67*, 3249; h) R. Bontchev, M. Nyman, unpublished results.
- [4] a) M. Nyman, F. Bonhomme, T. M. Alam, M. A. Rodriguez, B. R. Cherry, J. L. Krumhansl, T. M. Nenoff, A. M. Sattler, *Science* **2002**, *297*, 996; b) M. Nyman, F. Bonhomme, T. M. Alam, J. B. Parise, G. M. B. Vaughan, *Angew. Chem.* **2004**, *116*, 2847; *Angew. Chem. Int. Ed.* **2004**, *43*, 2787; c) F. Bonhomme, J. P. Larentzos, T. M. Alam, E. J. Maginn, M. Myman, *Inorg. Chem.* **2005**, *44*, 1774; d) M. Nyman, A. J. Celestian, J. B. Parise, G. P. Holland, T. M. Alam, *Inorg. Chem.* **2006**, *45*, 1043.
- [5] a) E. J. Graeber, B. Morosin, *Acta Crystallogr. Sect. B* **1977**, *33*, 2137; b) M. Nyman, L. Criscenti, F. Bonhomme, M. A. Rodriguez, R. T. Cygan, *J. Solid State Chem.* **2003**, *176*, 111; c) M. Maekawa, Y. Ozawa, A. Yagasaki, *Inorg. Chem.*, DOI: 10.1021/ic0601788.
- [6] a) J. T. Rhule, C. L. Hill, D. A. Judd, *Chem. Rev.* **1998**, *98*, 327; b) M. H. Dickman, M. T. Pope, *Inorg. Chem.* **2001**, *40*, 2582; c) M. H. Cjoang, C. W. Williams, L. Soderholm, M. R. Antonio, *Eur. J. Inorg. Chem.* **2003**, *14*, 2663; d) A. J. Russell, J. A. Berberich, G. F. Drevon, R. R. Koepsel, *Annu. Rev. Biomed. Eng.* **2003**, *5*, 1.
- [7] a) Crystal structure data for **2**: crystal size $0.38 \times 0.37 \times 0.14 \text{ mm}^3$, triclinic, space group $P\bar{1}$ (no. 2), $a = 16.7734(10)$, $b = 20.6133(13)$, $c = 26.3179(16) \text{ Å}$, $\alpha = 112.520(1)$, $\beta = 102.932(1)$, $\gamma = 96.186(1)^\circ$, $V = 8001.1(8) \text{ Å}^3$, $Z = 2$, $\rho_{\text{calcd}} = 2.059 \text{ g cm}^{-3}$; diffractometer: Siemens SMART 1K CCD (MoK_α radiation $\lambda = 0.71073 \text{ Å}$, graphite monochromator), $\mu = 2.332 \text{ mm}^{-1}$; narrow-frame scan at $T = 293 \text{ K}$, $2\theta_{\text{max}} = 46.00^\circ$, 38657 measured reflections, 22126 independent reflections, the program SADABS^[8a] was used for the absorption correction; structure solved by direct methods and refined by least-squares methods on F^2 by using SHELXTL^[8b] 1490 free parameters; GOF = 1.004, R values ($I > 2\sigma(I)$): $R1 = 0.081$, $wR2 = 0.213$; max./min. residual electron density: $1.70/-0.55 \text{ e}^- \text{ Å}^{-3}$. CCDC 606228 contains the supplementary crystallographic data for this paper. These data can be obtained free of charge from The Cambridge Crystallographic Data Centre via www.ccdc.cam.ac.uk/data_request/cif.
- [8] a) G. M. Sheldrick, SADABS, v. 2.10. Program for Empirical Absorption Correction of Area Detector Data, University of Göttingen: Göttingen, Germany, **2003**; b) SHELX97 (Includes SHELXS97, SHELXL97, CIFTAB)—Programs for Crystal Structure Analysis (Release 97-2). Institut für Anorganische Chemie der Universität, Tammanstrasse 4, 3400 Göttingen, Germany, **1998**.
- [9] a) J. T. Lewandowski, I. J. Pickering, A. J. Jacobson, *Mater. Res. Bull.* **1992**, *27*, 981; b) J. L. Fourquet, C. Jacoboni, R. de Pape, *Mater. Res. Bull.* **1973**, *8*, 393.
- [10] I. D. Brown and D. Altermatt, *Acta Crystallogr. Sect. A* **1985**, *41*, 244.
- [11] a) F. J. Farell, V. A. Maroni, T. G. Spiro, *Inorg. Chem.* **1969**, *8*, 2638; b) M. Von Rainer, H. Bierbusse, J. Fuchs, *Z. Anorg. Allg. Chem.* **1971**, *385*, 230; c) C. Rocchiccioli-Deltcheff, R. Thouvenot, M. Dabbabi, *Spectrochim. Acta Part A* **1977**, *33*, 143.
- [12] a) M. I. Khan, *J. Solid State Chem.* **2000**, *152*, 105; b) M. I. Khan, E. Yohannes, D. Powell, *Inorg. Chem.* **1999**, *38*, 212; c) M. I. Khan, E. Yohannes, D. Powell, *Chem. Commun.* **1999**, 23; d) J. Lu, Y. Xu, N. K. Goh, L. S. Chia, *Chem. Commun.* **1999**, 832; e) J. Do, R. P. Bontchev, A. J. Jacobson, *Inorg. Chem.* **2000**, *39*, 4305.